Neural Maturation Provides the Stability of Representation and the Solution for Understanding Complex Concepts

Hiroyasu Watanabe
Bream Research Group

summary

Recent advancements in realizing human-like brain functions through artificial intelligence have progressed significantly day by day. However, much of this astonishing progress in AI does not necessarily require an understanding of modern molecular biology. Here, I illustrate the significance of neural maturation in neural network-based information processing models. In both supervised and reinforcement learning paradigms, immature transmission can learn properties like normal high-fidelity conditions but lose these properties after reaching catastrophic points. I then investigated genes responsible for neuronal maturation and found that the candidate gene KCNH7 is expressed at higher levels during mouse brain development. In the simulated neural model with the KCNH7 channel property, the excitation threshold increased, resulting in a linear response property. These properties enhanced the stability of representation recall and enabled the comprehension of complex concepts in unsupervised learning models.
These results highlight the importance of neural maturation in achieving higher recognition abilities in adults.

Acknowledgements

I am thankful for the kind support of Junichiro Yoshimoto for discussions and comments on my work. Hiroshi Watanabe and Atsuhito Toyomaki also provided comments and support for my work.

Declaration of Interests

The author declares no competing interests.

Recent technological progress in realizing human-like brain functions for recognizing objects, understanding natural language, and navigating behavior in systems like “self-driving cars,” provided by artificial intelligence, has made a huge impact on our lives. These technologies continue to progress day by day. The basic model concepts of these artificial intelligences were provided by theoretical examinations of brain functions (1). Most of these theoretical bases were proposed before the expansion of molecular biology, indicating that major

parts of the current astonishing progress in AI do not necessarily require an understanding of modern molecular biology.

There have been intense research efforts to reveal the molecular mechanisms of neuronal transmission “maturation” in neurophysiology, based on observations of developmental changes in the excitability of neurons through synaptic transmission. This is especially true for the Calyx of Held synapse, a brainstem relay neuron involved in hearing and sound localization (2). These changes collectively refine neural information delivery to higher processing regions of the brain (3-6). Because the function of the Calyx of Held is primarily the transmission of auditory information, a developmental shift towards “high fidelity” is certainly reasonable. At the same time, considering the general context of adult information processing compared to that of children, the hypothesis that neuronal transmission turns to high fidelity during development is quite generalizable in the brain.

Here, I examine the significance of neural maturation in neural network-based information processing models. I mimicked immature neural transmission in a typical MNIST dataset (https://yann.lecun.com/exdb/mnist/) for training neural network models. Immature transmission was simulated by adding a random function between the layer’s forward transmissions. In both supervised and reinforcement learning paradigms, immature transmission could learn properties like normal high-fidelity conditions before reaching catastrophe points. However, continuous long-term learning induced a loss of learning results.

Then I looked for genes with physiological significance for neuronal transmission fidelity. I focused on candidates from potassium channel genes. Through in situ hybridization data and single-cell RNA-Seq analysis, I found that the candidate gene KCNH7 is expressed at higher levels during the development of the mouse brain.

In the simulated neural model with the KCNH7 channel property, the excitation threshold increased, providing a linear response property instead of the binary one observed without the KCNH7 condition. These properties enhanced the stability of representation recall and further enabled the understanding of complex concepts.

These results demonstrate the significance of neural maturation in achieving higher recognition abilities in adults. Additionally, they may provide insights into understanding the mechanisms of psychiatric disorders.

Effect of pseudo-immature transmission in supervised learning of the MNIST dataset

I speculated on the possibility of examining the significance of neural transmission maturation in conventional deep learning networks. First, I examined this in three-layer networks using supervised learning for the MNIST dataset (Fig. 1). I utilized ReLU for the activation function. This model network could learn text concepts immediately and maintain stable accuracy over long trials (Fig. 1a). I simply modified the forward transmission by adding random values to reproduce immature low-fidelity neural transmissions. Fig. 1b showed that this condition could also learn the concept, albeit with slightly lower accuracy. However, as a result of continuous learning, the obtained learning representation suddenly dropped off and was lost. This change caused a divergence in neural firing values. Therefore, I next examined clipping the activation function values at a certain point, such as limiting values over 500 to 500. Fig. 1c showed almost the same results as Fig. 1b. The last layer is directly converted to 0-9 text output. During the divergence of the value, when the true and false output layer values reached the limiting value, backpropagation couldn't recover the mismatch of input-output relations (data not shown).

Fig. 1d and 1e show the results of random transmission with optimized learning rates using Adam. I needed to adjust the learning rate lower than in the condition without Adam to maintain stable accuracy, but random transmission lost the stability of concept learning in the same way as the control condition. Fig. 1f and 1g show the results of utilizing random dropout. I also adjusted the learning rate slightly higher, but this condition yielded the same results as Fig. 1a and Fig.1b.

Divergence of action values in 3x4 grid world reinforcement learning

I examined the effects of random transmission in the reinforcement learning paradigm. I performed Q-Learning in a 3x4 grid world using a single-layer network. Fig. 2a shows the results of learning with the ReLU activation function. Compared with Fig. 2g (Step function), ReLU could have negative values, showing a higher variation of action functions. However, the ReLU function condition diverges the action function value due to random transmission (Fig. 2b). In the gradient clipping conditions, limiting the gradient value at the set value, gradient divergence could be controlled even with random transmission, but the learning of action was completely inappropriate for achieving better navigation for the task (Fig. 2d).

In the case where ReLU activation function values over 10 are set to 0, causing the action function value to diverge nevertheless without adding randomness (Fig. 2e). This was not observed when the value was clipped constantly (Fig. 2f). The condition where values over 50 are set to 0 did not induce the action function values to diverge (data not shown).

On the other hand, in the Step function conditions (Fig. 2h), action function divergence was not observed even with random transmission. These results show that the ReLU type function is highly expressive but at the same time vulnerable to perturbations, whereas binary response functions are more stable.

KCNH7 - A candidate gene with higher expression in the mature mouse brain

I looked for a real molecular target contributing to neural firing fidelity. The simplest working hypothesis is that these genes would be expressed at higher levels in the adult brain compared to the immature brain. I searched for such potassium channels using the ALLEN BRAIN ATLAS DATA PORTAL (https://portal.brain-map.org/). From the in situ hybridization data of the developing mouse brain, I identified several candidates (Fig. 3a). Through the examination of the cell type database by single-cell RNA-Seq analysis (Fig. 3b), I selected KCNH7 as a good candidate.

The KCNH family comprises the ERG, EAG, and ELK voltage-activated, potassium-selective channels, and KCNH7 belongs to the ERG (Kv11) subfamily. These channels were originally identified as mutations in Drosophila that exhibited abnormalities under ether anesthesia (7). Due to their unique channel properties, Kv11 channels evoke greater conductance by hyperpolarization from depolarized potentials and regulate the resting membrane potential and action potential firing in neurons (8-10).

According to the in situ hybridization data, KCNH7 starts to express at higher levels after P14 in the mouse telencephalic vesicle, midbrain, and medullary hindbrain (Fig. 3a). Fig. 3b shows samples from the P28 mouse brain, where KCNH7 is widely expressed throughout the cortex in both excitatory and inhibitory neurons. However, expression is partially low in some populations of CA3 and dentate gyrus neurons. In these cell types, the immature neuron marker Calbindin2 (Calretinin) is negatively correlated with KCNH7 expression, while the mature neuron marker Calbindin1 is positively correlated with KCNH7 expression (Fig. 3c) (11, 12). These results provide evidence for the potential importance of KCNH7 in adult neuron function.

Next, I examined the functions of KCNH7 in neurons. I utilized established neuron models by incorporating KCNH7 parameters. Niculescu et al. demonstrated the feasibility of inputting KCNH7 model parameters into a modified KGR model (10). I checked the channel kinetics through examinations such as activation and deactivation kinetics. My Hodgkin-Huxley-based model appeared to sufficiently reproduce the trends of KCNH7 parameters (Supplemental Table).

Modified KGR models utilized in Niculescu et al. start to fire in a binary manner, meaning that adding threshold current induces continuous firing during the duration time (Fig. 4a). An increase in potassium channel conductance in the model induced a higher threshold in the neuron model, but the binary firing property remained unchanged (Fig. 4b). When KCNH7 model parameters were incorporated into this neuron model, the first firing threshold became higher, similar to the high potassium channel conductance model. The results showed that KCNH7 strongly repressed the second firing, resulting in a continuous increase in the duration time of firing (Fig. 4c). This property aligns well with the reported physiological function of KCNH7 (10).

This property could provide neural transmission fidelity in cases where transmission current varied near the set firing points (Fig. 4d left). The model including KCNH7 showed the same single action potential response even when slight perturbations occurred. One of the KCNH7 SNPs has been reported to be related to bipolar spectrum disorder (13). This amino acid replacement mutation shifts the KCNH7 $V_{1/2}$ values to about +10mV higher threshold. This mutation parameter appears to partially block the KCNH7 function (Fig. 4d right) and provides insights into understanding the phenotype of this SNP.

I examined the above hypothesis through the activation of neurons by Poisson spike noise (Fig. 4e). I confirmed that KCNH7 suppressed variance caused by noise compared to the original model. This effect was partially impaired by the KCNH7 mutation. The high K channel conductance model also provided a similar effect, showing that the high threshold induced by these channels is important for stability under noise perturbation conditions.

Then I examined the function of KCNH7 during high firing rate stimulation (Fig. 4f). The control neuron model couldn’t maintain action potential firing at 530 Hz. Both the high conductance potassium channel and KCNH7 conditions maintained action potential firing at 530 Hz. KCNH7 showed a higher ability to sustain maximum firing response (150 Hz) even with high-frequency stimulation compared to the others.

Effects of neuronal threshold in unsupervised learning of spiking neural network

I examined the significance of the property provided by KCNH7, which shifts the activation threshold higher, in a spiking neural network model using the STDP learning algorithm (14) (Fig. 5). The original development model is very stable even with long trial learning, as described in their work (Fig. 5 (a), (b); control).

I perturbed the model by increasing the learning rate. Even under normal threshold conditions, the learned association firing was periodically lost during continuous learning. In low threshold conditions, where both excitatory and inhibitory neurons fire easily, this trend of learning loss increased further. On the other hand, the periodic drop in learning was partially suppressed in high threshold conditions (Fig. 5c, 5d). The difference is statistically significant ($p < 0.05$) (Fig. 5d).

These results potentially showed that the high threshold properties of neurons, achieved by increasing KCNH7 expression, provided stability for learning concepts.

Effects of randomness in Restricted Boltzmann Machine

I examined the effect of randomness in unsupervised association learning using a Restricted Boltzmann Machine to generate the numbers of the MNIST dataset. I parameterized the temperature factor by dividing the sigmoid variable by the set temperature factor to control the randomness of information transmission during learning. Fig. 6a, b, and c show the results of character “5” concept learning and recalling by giving the test images. In this condition, ($t = 1$) (normal sigmoid function) was optimal (Fig. 6a). In low temperature conditions ($t = 1/4$), which induced binary-like activation, convergence was clearly fast (Fig. 6b). In high temperature and high randomness conditions ($t = 4$), the sigmoid was converted to a nearly linear function, where convergence was slow and divergence also occurred in some trials (Fig. 6c). These results are consistent with those in Fig. 1.

However, when using the same paradigm for learning the characters “5” and “1,” the convergence properties of the pair of numbers were opposite to the results above. In low temperature conditions ($t = 1/4$), convergence was still very quick, but although the two-character concepts could be obtained initially, the learning concepts were rapidly lost, and eventually, only one character could

be recalled (Fig. 6d). In 16 out of 150 tests, the maximum values reached over 0.6 accuracy, reflecting the ability to recall 2 characters, but in 0 tests did the accuracy remain over 0.6 at the last 400,000 epochs. This clearly showed a divergence of the concept. In high temperature conditions (t = 4), the two-character concepts gained higher accuracy as more trials were added. In 25 out of 150 tests, the maximum values reached over 0.6 accuracy, and in 22 tests, the accuracy remained over 0.6 at the last 400,000 epochs. These results show continuous convergence of the correct concepts. In the (t = 1) condition, 43 out of 150 tests had maximum values reaching over 0.6 accuracy, but only 15 tests maintained over 0.6 accuracy at the last 400,000 trials. These results showed that (t = 1) was still optimal for fitting the concept of two characters initially, but during continuous learning, the correct two-character concept was gradually lost.

Taken together, the results suggest that the linear response property provided by adding KCNH7 induces a higher capacity for complex information processing in neuronal function.

Discussion

Both supervised learning and reinforcement learning models showed that continuous learning trials under random conditions induced a loss of learning (Fig. 1, Fig. 2). These losses were caused by the divergence of activation values. However, even when setting a limit on the activation value, similar to physiological neurons, these phenomena were still observed (Fig. 1c, Fig. 2). Additionally, Fig. 2d showed that learning loss was still observed even when setting limits on the gradient. Fig. 2e and 2f suggest that firing failure has a more severe effect on learning establishment than maintaining maximal response frequency. The expression of KCNH7 could rescue this limitation of learning (Fig. 4f).

It seems that catastrophic forgetting is consistent with our results (15). It is induced by adding perturbations in learning sources, such as adding randomness in learning images. It is a straightforward interpretation that randomness in learning sources and transmission would have similar effects.

Fig. 2 shows that learning loss due to randomness occurred only in the ReLU condition. It was also observed in supervised learning (data not shown). In the case of the step function (Fig. 2g), learning losses were not observed.

Regarding the complexities of learned behavior, ReLU had a higher variety of behavior possibilities. It could even learn “minus” parameters (Fig. 2a,

shown in red). On the other hand, the step function only chose 0 or 1. Even with such low expression ability, the step function worked well and appeared to perform better than ReLU in this simple task and was at least clearly more robust to perturbations than ReLU. The same results could be obtained in the Restricted Boltzmann Machine model (Fig. 6a, 6b, 6c). In high temperature/high randomness conditions, the learning tended to lose its ability through continuous learning (Fig. 6c).

On the other hand, when the same Restricted Boltzmann Machine model learned a more complex context, the phenotype of learning loss became opposite. Low temperature conditions induced learning loss, while high temperature conditions provided stable, continuous improvement in learning accuracy (Fig. 6d, 6e, 6f).

These results provide a reasonable interpretation for the higher expression of KCNH7 in mature neurons (Fig. 3a). KCNH7 provides a continuous linear response and a higher threshold for neurons (Fig. 4c). In short, higher thresholds provide stability (Fig. 4e) in learning (Fig. 5), and the complexity of responses gives the ability to handle complex problems (Fig. 6f). This could be seen as a simple expression of the maturation of intelligence in the adult brain, and moreover, it provides valuable insights into how to utilize such higher abilities in organizations and society.

Chronic treatments of adult mice with fluoxetine induce “dematuration” of mature granule cells through activation of 5HT-4 receptors (16). 5HT-4 receptors are known Gs-coupled receptors that activate PKA (17). Another group shows that 5HT-4 also activates PKC alpha in intestinal epithelial cells (18).

mGluR1, a Gq-coupled receptor, activation in Purkinje cells induces suppression of KCNH7 current, as measured by adding the ERG current inhibitor E4031, promoting excitation of neurons (10). This would disturb information stability as discussed here (Fig. 4e, Fig. 5). Activation of mGluR1 coincidentally induced about a +10mV shift of KCNH7 $V_{1/2}$. This might be the endogenous regulatory mechanism of KCNH7 through PKC phosphorylation. Indeed, KCNH7 is phosphorylated by PKC according to the KANPHOS database (https://kanphos.jp/).

Artificial intelligence is, of course, “artificial,” but recent progress in these technologies has already accomplished most human cognitive functions. The fact that most cognitive functions can be performed means that most cognitive functions can be approximately examined. Insights from AI can provide cues

for understanding the significance of molecular mechanism dynamics in cognitive function, as shown here. My study is quite simple, and primitive compared to the deeper understanding of cognitive function mechanisms. Now, it is possible to build more sophisticated architectures of neural networks and to examine the same types of problems, surely making a huge breakthrough in the field.

Referecnce

1. Amari S. 1993. Backpropagation and stochastic gradient descent method. Neurocomputing, 5 (4–5) , 185-196.
2. Takahashi T. 2015. Strength and precision of neurotransmission at mammalian presynaptic terminals. Proceedings of the Japan Academy, Series B, 91(70), 305-320.
3. Koike-Tani M, Saitoh N, Takahashi T. 2005. Mechanisms Underlying Developmental Speeding in AMPA-EPSC Decay Time at the Calyx of Held. J Neurosci., **25**(1), 199-207.
4. Taschenberger H and von Gersdorff H. 2000. Fine-Tuning an Auditory Synapse for Speed and Fidelity: Developmental Changes in Presynaptic Waveform, EPSC Kinetics, and Synaptic Plasticity. J neurosci., **20**(24), 9162-73.
5. Yamashita T, Eguchi K, Saitoh N, von Gersdorff H, Takahashi T. 2010. Developmental shift to a mechanism of synaptic vesicle endocytosis requiring nanodomain Ca2+. Nat Neurosci., **13**(7), 838–844.
6. Yang YM and Wang LY. 2006. Amplitude and Kinetics of Action Potential-Evoked Ca2+ Current and Its Efficacy in Triggering Transmitter Release at the Developing Calyx of Held Synapse. J Neurosci., **26**(21), 5698–5708.
7. Brüggemann A, Pardo LA, Stühmer W, Pongs O. 1993. Ether-à-go-go encodes a voltage-gated channel permeable to K+ and Ca2+ and modulated by cAMP. Nature, **365**(6445), 445-8.
8. Perry M, Sanguinetti M, Mitcheson J. 2010. Revealing the structural basis of action of hERG potassium channel activators and blockers. J Physiol., 2010 **588**(Pt 17), 3157-67
9. Akbarali HI, Thatte H, He XD, Giles WR, Goyal RK. 1999. Role of HERG-like K(+) currents in opossum esophageal circular smooth muscle. Am J Physiol., **277**(6), C1284-90.
10. Niculescu D, Hirdes W, Hornig W, Pongs O, Schwarz JR. 2013. Erg Potassium Currents of Neonatal Mouse Purkinje Cells Exhibit Fast Gating Kinetics and Are Inhibited by mGluR1 Activation. J Neurosci., **33**(42), 16729-40.
11. Iacopino AM, Rhoten WB, Christakos S. 1990. Calcium binding protein (calbindin-D28k) gene expression in the developing and aging mouse cerebellum. Brain Res Mol Brain Res., **8**(4), 283-90.

12. Brandt MD, Jessberger S, Steiner B, Kronenberg G, Reuter K, Bick-Sander A, von der Behrens W, Kempermann G. 2003. Transient calretinin expression defines early postmitotic step of neuronal differentiation in adult hippocampal neurogenesis of mice. Mol Cell Neurosci., **24**(3), 603-13.
13. Strauss KA, Markx S, Georgi B, Paul SM, Jinks RN, Hoshi T, McDonald A, First MB, Liu W, Benkert AR, Heaps AD, Tian Y, Chakravarti A, Bucan M, Puffenberger EG. 2014. A population-based study of KCNH7 p.Arg394His and bipolar spectrum disorder. Mol Genet., **23**(23), 6395-406.
14. Diehl PU, Cook M. 2015. Unsupervised learning of digit recognition using spike-timing-dependent plasticity. Front Comput Neurosci., 9:99.
15. Kirkpatricka J, Pascanua R, Rabinowitza N, Venessa J, Desjardinsa G, Rusua AA, Milana K, Quana J, Ramalhoa T, Grabska-Barwinskaa A, Hassabisa D, Clopathb C, Kumarana D, Hadsella R. 2017. Overcoming catastrophic forgetting in neural networks. Proc Natl Acad Sci USA, **114** (13), 3521-3526.
16. Kobayashi K, Ikeda Y, Sakai A, Yamasaki N, Haneda E, Miyakawa T, Suzuki H. 2010. Reversal of hippocampal neuronal maturation by serotonergic antidepressants. Proc Natl Acad Sci USA., **107**(18), 8434-9.
17. Torres GE, Arfken CL, Andrade R. 1996. 5-Hydroxytryptamine4 receptors reduce afterhyperpolarization in hippocampus by inhibiting calcium-induced calcium release5-Hydroxytryptamine4 receptors reduce afterhyperpolarization in hippocampus by inhibiting calcium-induced calcium release. Mol Pharmacol., **50**(5), 1316-22.
18. Gill RK, Saksena S, Tyagi S, Alrefai WA, Malakooti J, Sarwar Z, Turner JR, Ramaswamy K, Dudeja PK. 2005. Serotonin inhibits Na+/H+ exchange activity via 5-HT4 receptors and activation of PKCα in human intestinal epithelial cells. Gastroenterology, **128**(4), 962-74.
19. Kozareva V , Martin C, Osorno T, Rudolph S , Guo C , Vanderburg, Nadaf N, Regev A, Regehr WG, Macosko E. 2021. A transcriptomic atlas of mouse cerebellar cortex comprehensively defines cell types. Nature, **598**(7879), 214-219.

Figure 1: Effects of Random transmission in supervised learning of MNIST dataset

The MNIST text recognition task was performed using a typical deep layer network for supervised learning. The green line shows the accuracy of recognition (left vertical axis), and the orange line shows the loss value (right vertical axis). The horizontal axis shows the iteration numbers.(a) Control. The learning rate is 0.1. (b) Random forward(Pseudo-immature) transmission. (c)Random transmission with ReLU activation value was clipped at 500. (d) Using Adam optimization and with random transmission (e). The learning rate is 0.001. (f) Using random dropout and with random transmission (g). The learning rate is 0.2.

Figure 2: Effects of Random transmission in Q-Learning
3x4 maze tasks were performed using Q-Learning. Briefly, the agent starts from the bottom left block and chooses the next action based on the expectation value. If the agent hits the wall, it stays in place without incurring a penalty. When the agent reaches the goal reward point, it returns to the starting point and begins the next episode. The vertical axis shows the loss value, and the horizontal axis shows the episode numbers. The subplot shows the value of actions chosen in each block and the typical action directions for the next steps.(a) Activation function was ReLU. The activation function values was clipped at 50 for avoiding gradient explosion. (b) Random forward transmission with ReLU. (c) Gradient max value clipped at 5 and its random transmission(d). (e) ReLU activation values over 10 are set to 0, or 10 (f). (g)Step function and with random transmission (h).

Figure 3: A candidate gene with higher expression in the mature mouse brain Explore develop dependent up-regulating potassium channels in ALLEN BRAIN MAP. (a) In situ hybridization of mouse brain in each developmental stage and regions(https://developingmouse.brain-map.org/gene/show/82041). Vertical axis shows developmental stage, E11.5, E13.5, E15.5, E18.5, P4, P14 and P28. Horizontal axis shows brain regions, RSP, Tel, PedHy, p3, p2, p1, M, PPH, PH, PMH and MH. Right shows in situ hybridization of KCNH7 in P14 and P56 mouse cerebellum. As showed previously, KCNH7 was seen only expressed in Purkinje cell. (19) (b) Single cell RNA-Seq analysis of adult, P28, mouse brain.(https://celltypes.brain-map.org/rnaseq/mouse_ctx-hpf_10x?selectedVisualization=Heatmap&colorByFeature=Cell+Type&colorByFeatureValue=Gad1) (c) The white dashed line area in (b) shows KCNH7 expression in hippocampal neurons.

Figure 4: Functions of KCNH7 for neural fidelity

Examine the effects of KCNH7 parameter insertion in Purkinje cell model. Neuron models were stimulated from 300ms to 800ms at indicated amplitudes. (a) The threshold point for firing in the original model. (b) Increased potassium channel conductance in the model.(c) Inserted KCNH7 parameter as reported previously.

(d) Comparison of KCNH7 and pseudo-mutant with a +10mV higher V half, near the thresholds. (e) Effect of random noise. Each simulation model was added Poisson spikes and noise. The upper part shows the example of responses of the spikes. The lower part shows the mean values of frequency and variance from 50 seed trials. Except between KCNH7 and High K, all pairs showed statistically significant differences in both. The error bars are shown in the figure. (f) Comparison of the above three neurons under 10, 150, 300, and 530 Hz action potential-like stimulation.

Figure 5: Effects of High Threshold in a Spiking Neural Network Model
The vertical axis represents the proportion of concordant firing neurons between the training and test sessions, while the horizontal axis denotes the number of trials. (a) Learning rate (Lr) = 0.1. The control condition represents the optimal setting from the original paper, with a threshold 10 times higher than the original. (b) Lr = 0.07 with different weight parameters. (c) Lr = 0.07, tested every 10,000 trials. (d) Lr = 0.07, tested every 1,000 trials.

Figure 6: Effects of KCNH7 function in Restricted Boltzmann Machine model Numeric text recall from the MNIST dataset by a Restricted Boltzmann Machine. Temperature parameters in both forward transmission and random sampling were set to 1 (a), 1/4 (b), and 4 (c). The accuracy of text recall was calculated by the trained supervised learning network in Fig. 1. The vertical axis shows accuracy, and the horizontal axis shows the number of test trials (5000 epochs of additional learning in each trial, totaling 400,000 epochs). The right shows sigmoid shapes (blue) and firing probabilities of sampling (orange) for each t and x value. (d), (e), and (f) show the results of learning pair of numbers (5 and 1) and examples of generated characters. I selected data that achieved over 0.6 accuracy at the maximum during the trial. (g) The examples of generative characters in (e). Initially, two character concepts were obtained but were lost through continuous learning trials (left and center). The right image shows an example where one character concept was obtained. (h) The examples of generative characters in (f) showing two character concepts obtained.

Figure 1: Effects of Random transmission in supervised learning of MNIST dataset

(a) Control : Lr = 0.1

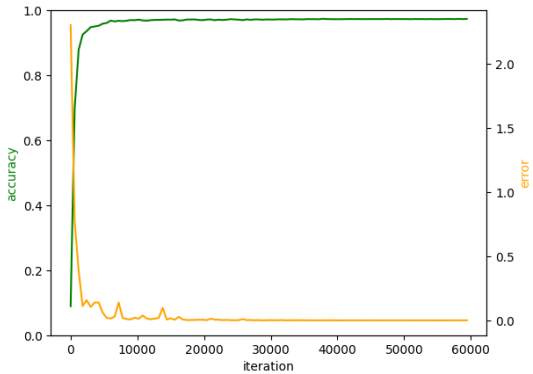

(b) Random : Lr = 0.1

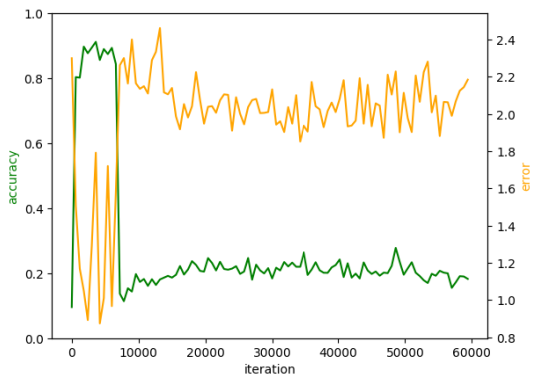

(c) Clip @500

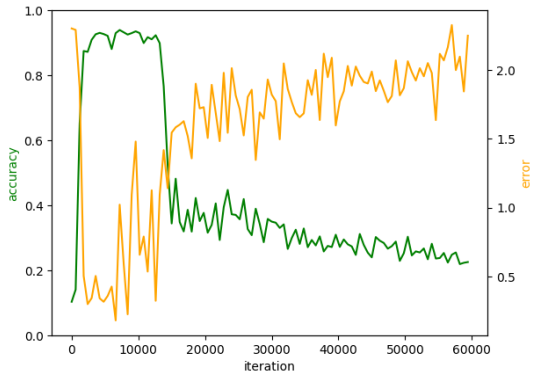

(d) Control(Adam) : Lr = 0.001

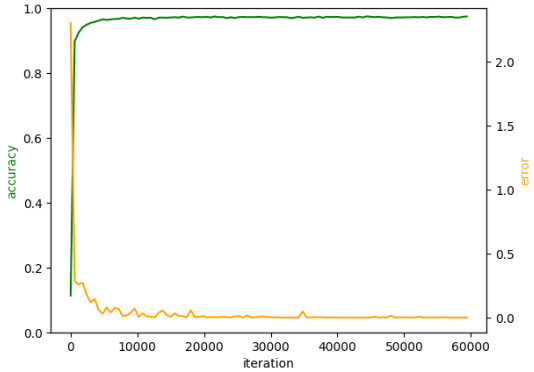

(e) Random(Adam) : Lr = 0.001

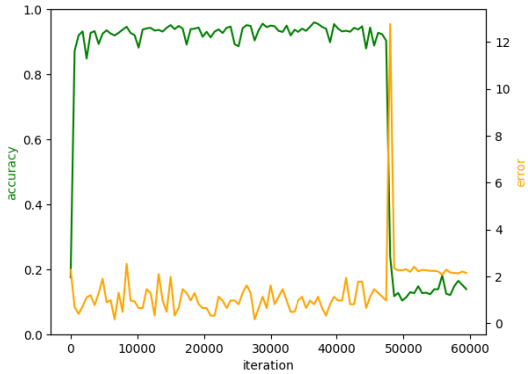

(f) Control(Dropout) : Lr = 0.2

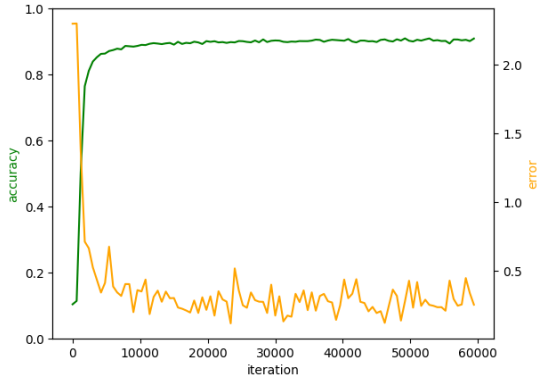

(g) Random(Dropout) : Lr = 0.2

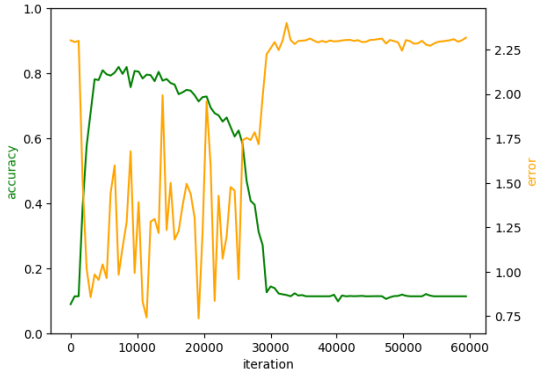

Figure 2: Effects of Random transmission in Q-Learning

(a) Control

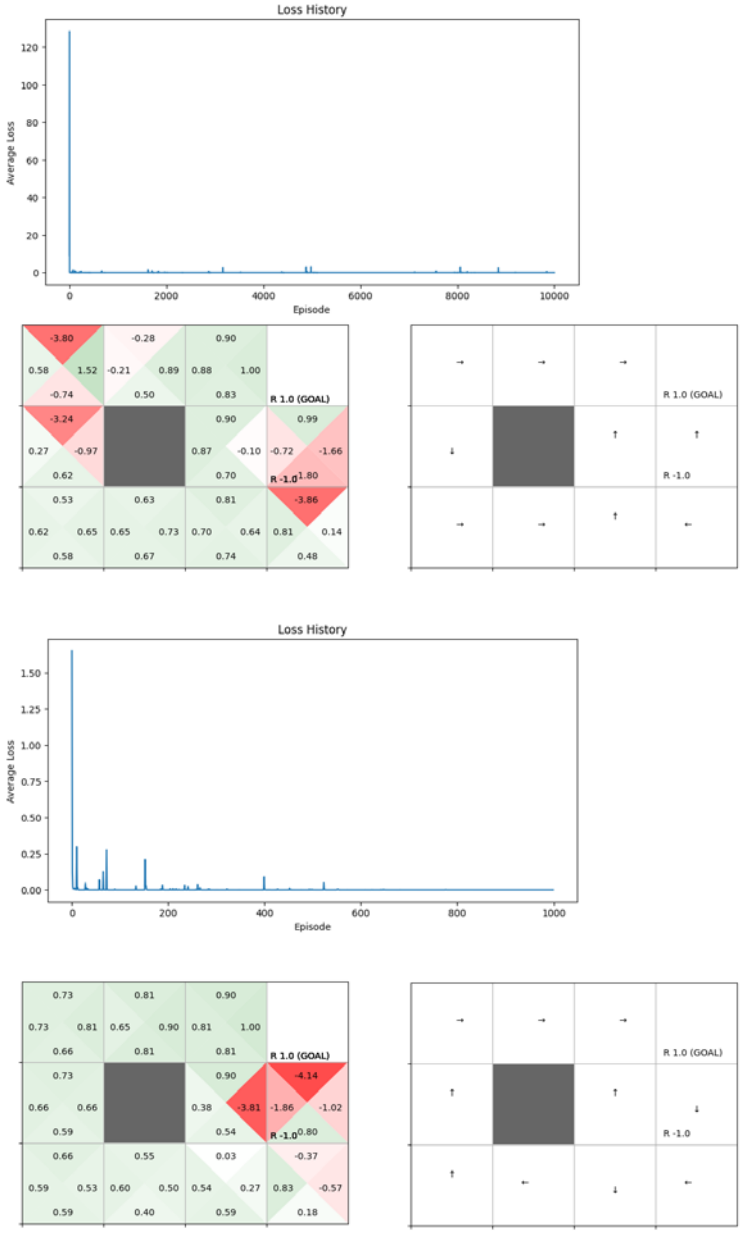

(b) Random

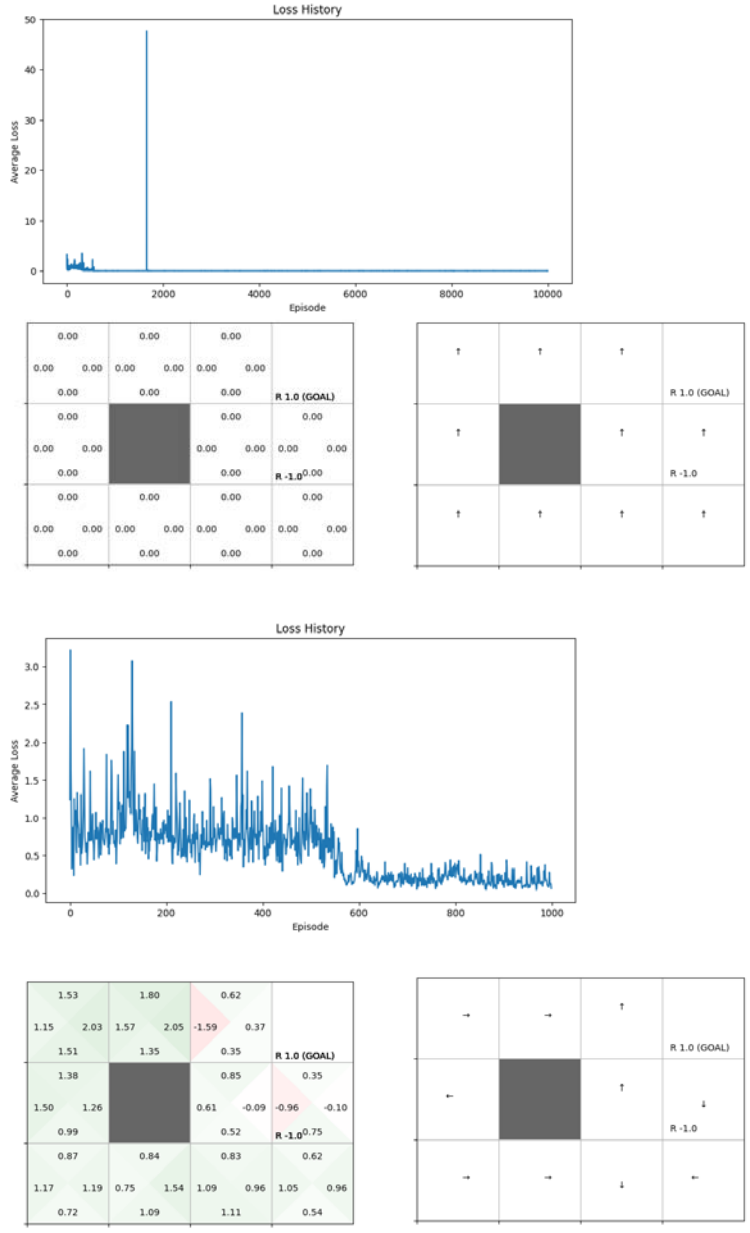

(c) Grad clipping

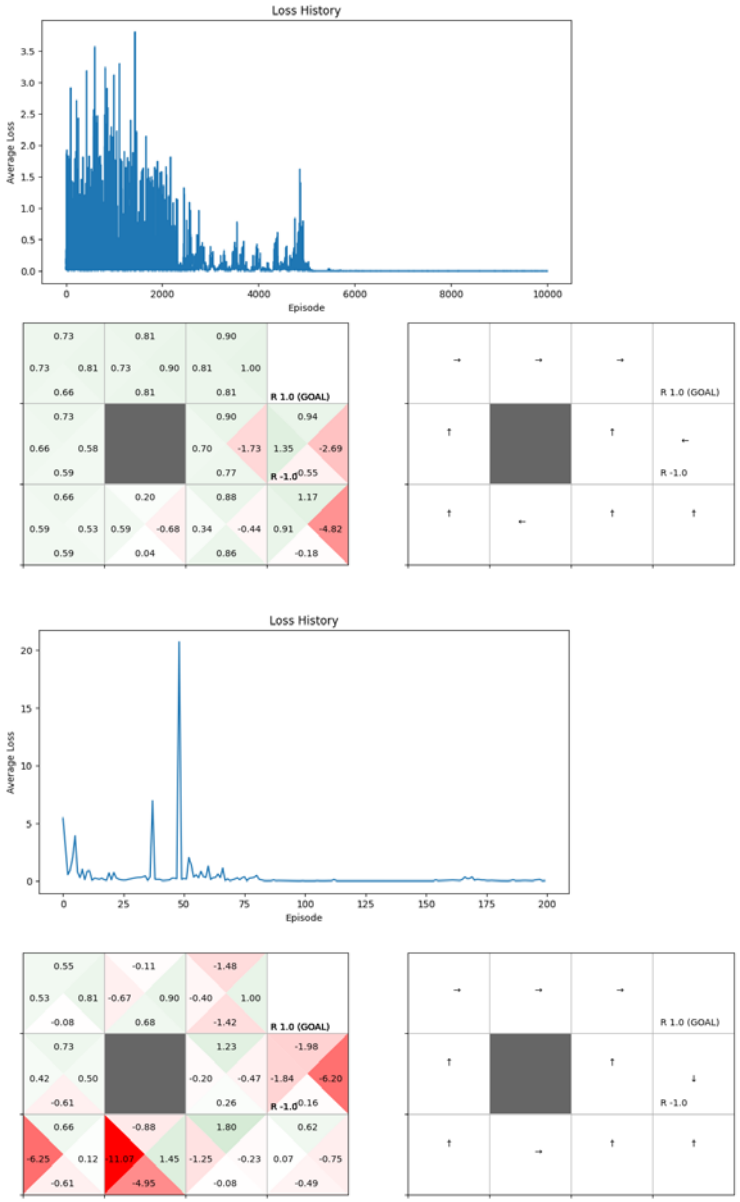

(d) Grad clipping + Random

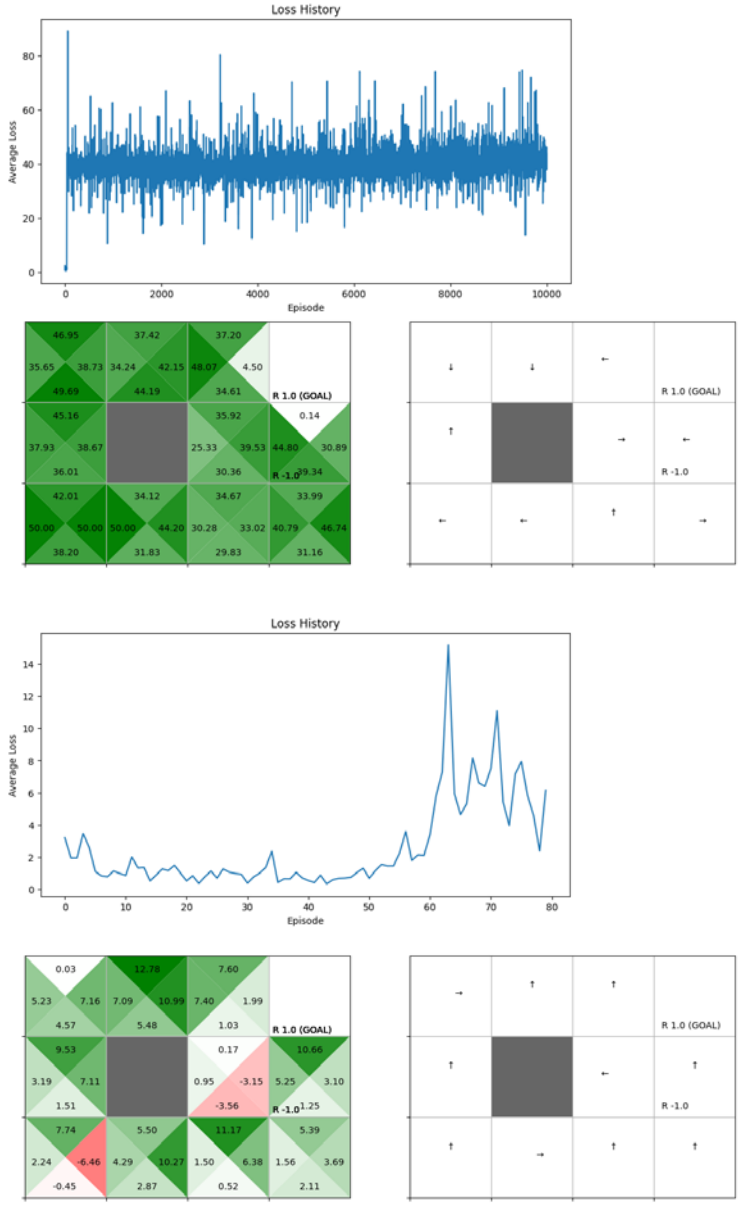

(e) ReLU 10 > 0

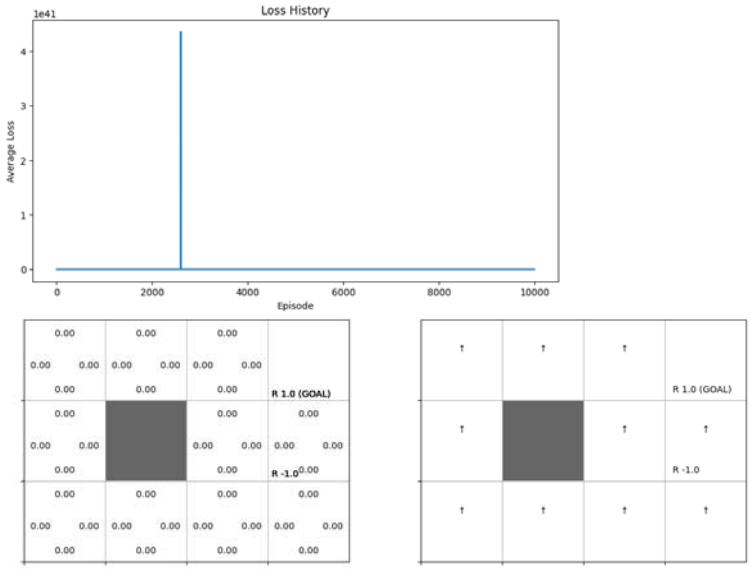

(f) ReLU 10 > 10

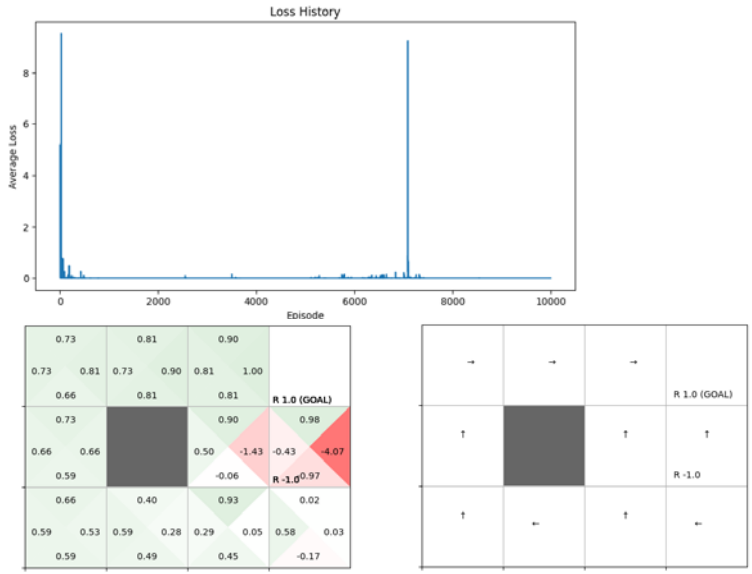

(g) Step

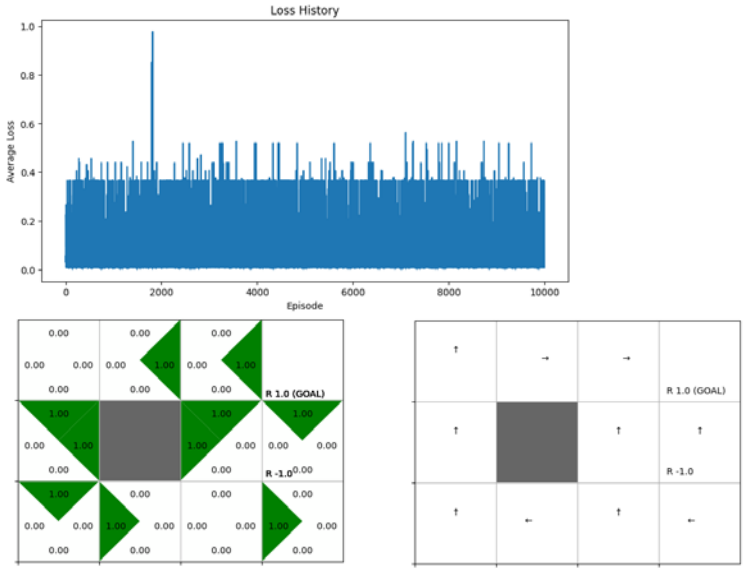

(h) Step + Random

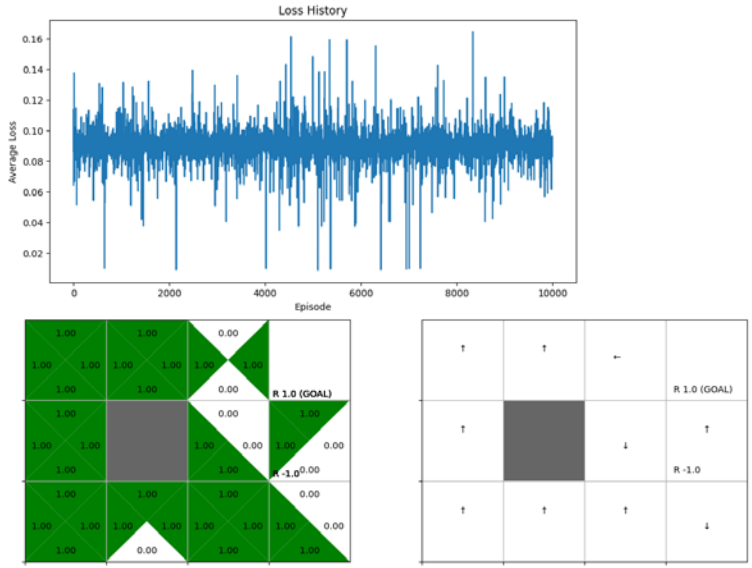

Figure 3: Candidate potassium channels expressed at higher levels in mature neurons

(a) In situ hybridization

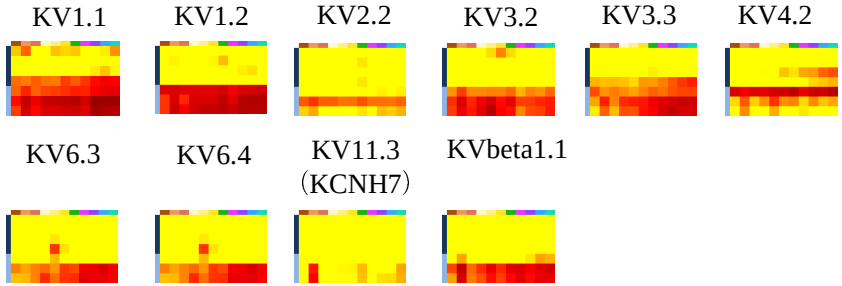

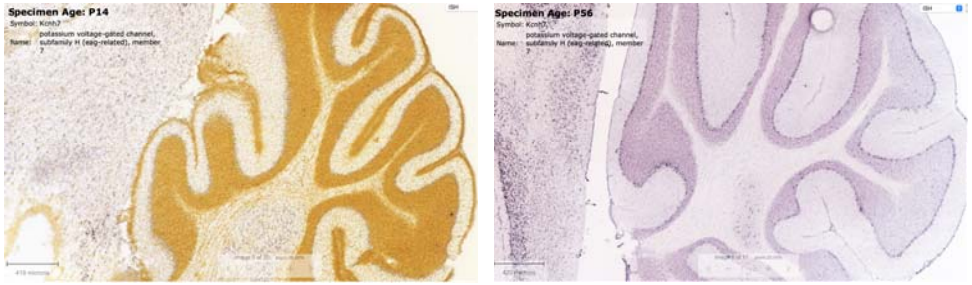

(b) Single cell RNA-Seq Analysis of Adult Mouse brain

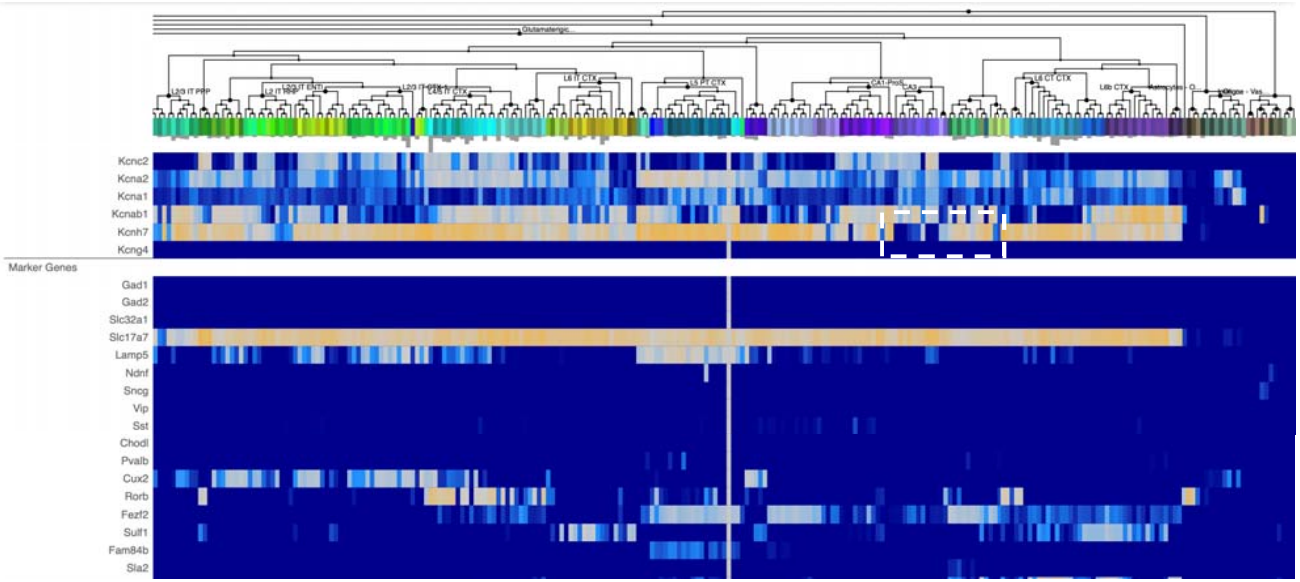

(c) Single cell RNA-Seq Analysis of hippocampal neuron

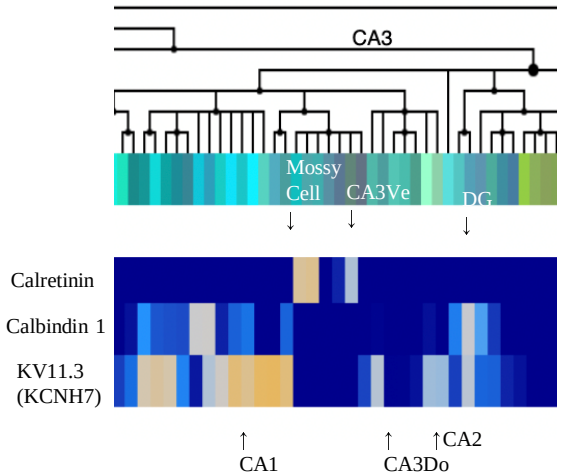

Figure 4: Functions of KCNH7 for neural fidelity

(a) Purkinje model original:
8.11pA(300-800ms)

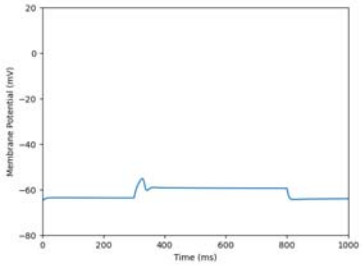

Purkinje model original:
8.12pA(300-800ms)

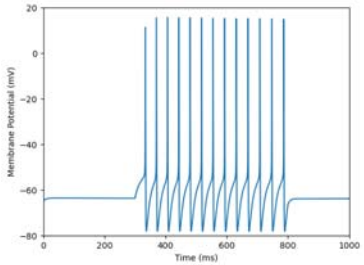

(b) High K conductance:
15.81pA(300-800ms)

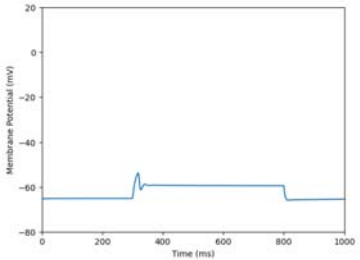

High K conductance:
15.82pA(300-800ms)

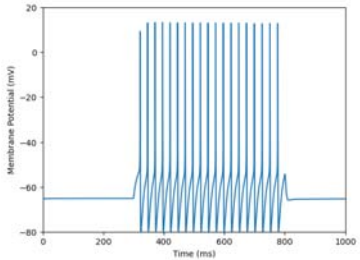

(c) +KCNH7:
13.2pA(300-800ms)

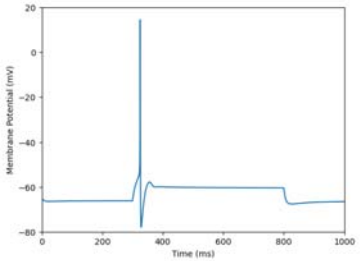

+KCNH7:
15pA(300-800ms)

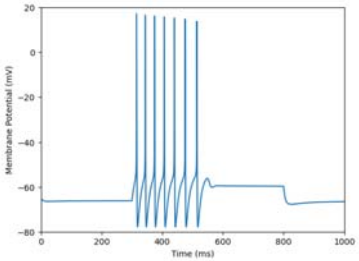

+KCNH7:
15.4pA(300-800ms)

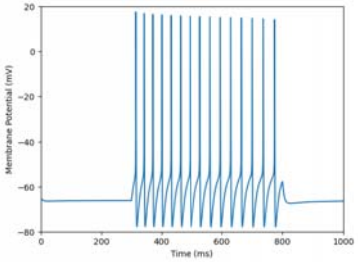

(d) KCNH7 or KCNH7 mut ($V_{1/2}$ + 10mV)

KCNH7:
13.2pA

KCNH7 mut:
11.2pA

Start point of firing

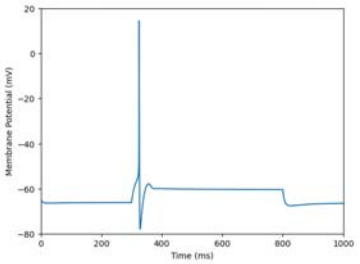

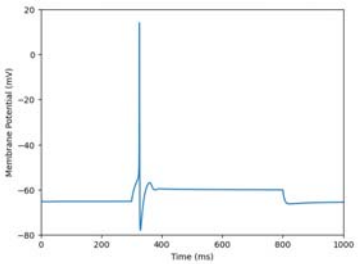

+0.5pA

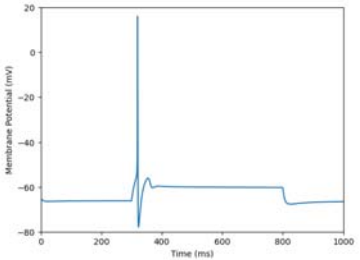

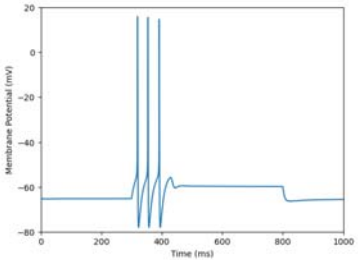

(e) Effect of noise in the models

Original

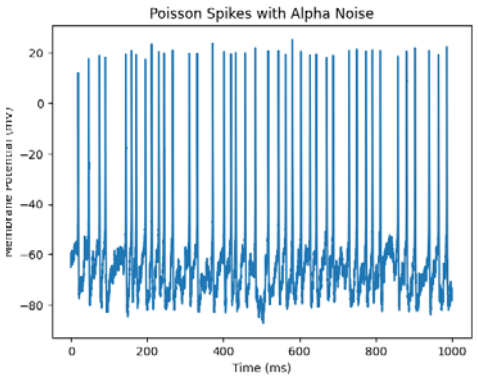

KCNH7

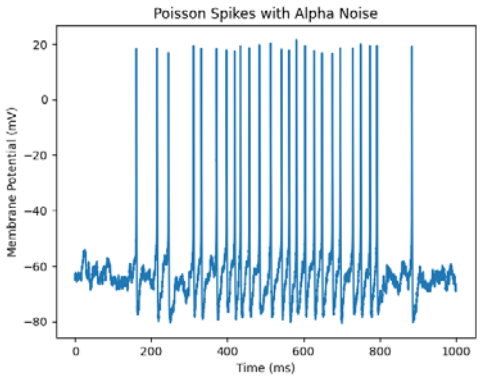

KCNH7 mut

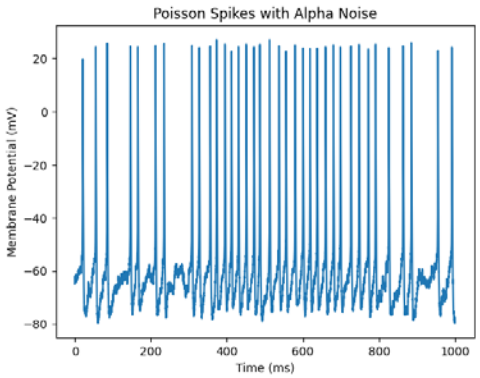

High K

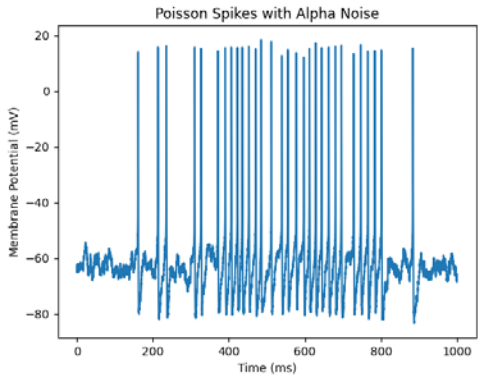

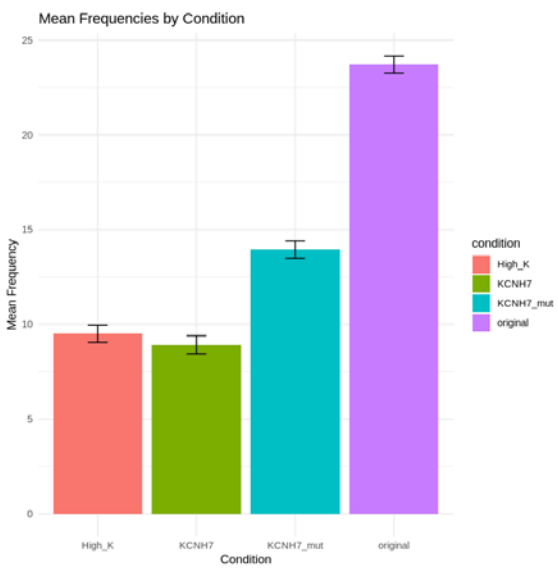

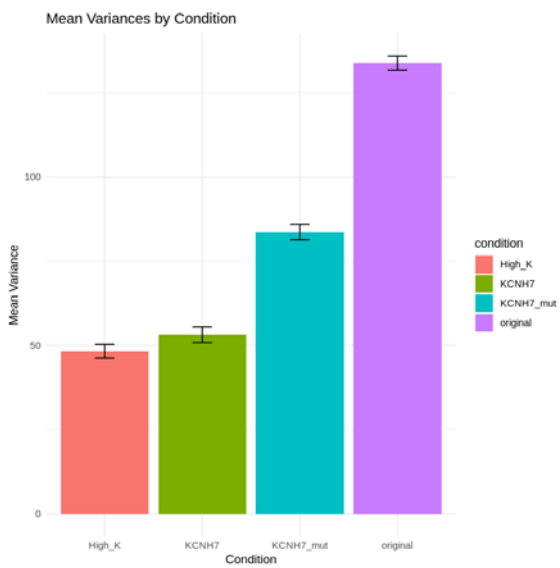

(f) KCNH7 suppresses failing of action potential

Original

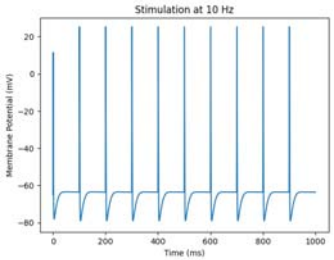

Frequency:10.00Hz

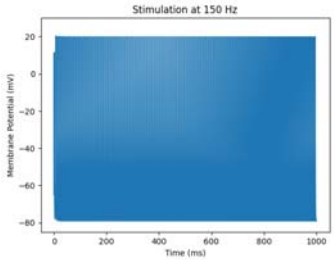

Frequency:149.95Hz

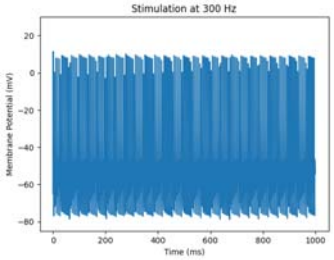

Frequency:164.09Hz

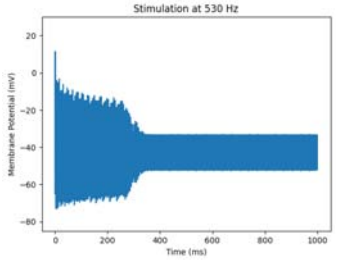

Frequency:192.48Hz

High K

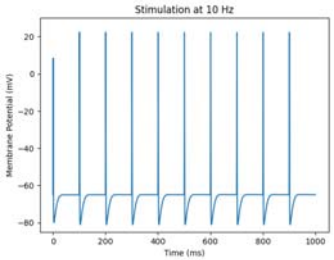

Frequency:10.00Hz

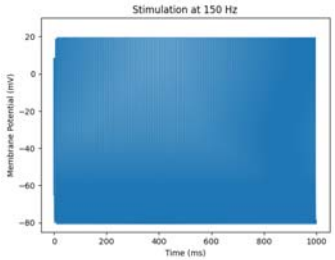

Frequency:149.95Hz

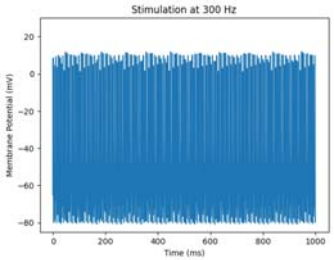

Frequency:182.57Hz

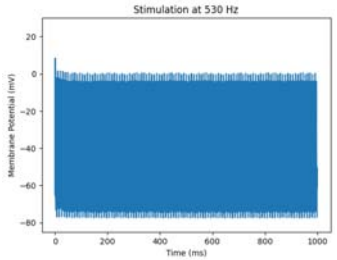

Frequency:212.03Hz

KCNH7

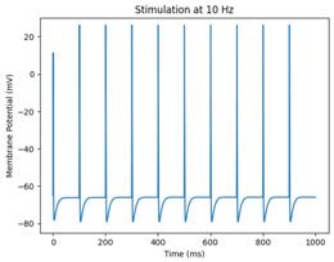

Frequency:10.00Hz

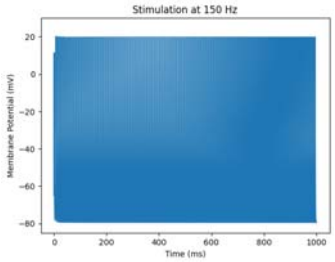

Frequency:149.95Hz

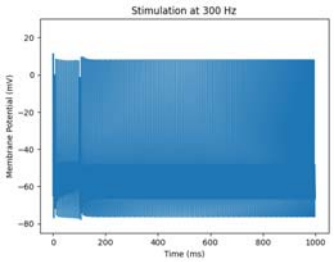

Frequency:150.99Hz

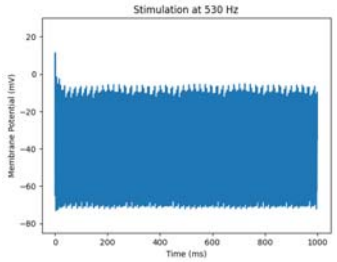

Frequency:198.31Hz

Figure 5: Effects of high threshold in spiking neural network model

(a) Lr = 0.1

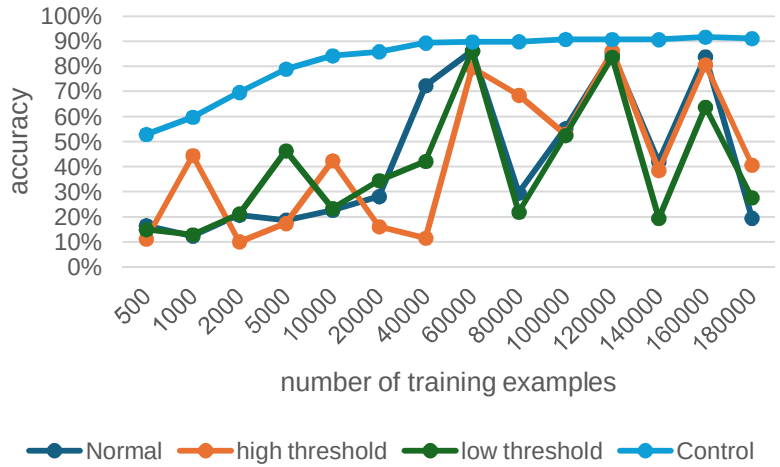

(b) Lr = 0.07

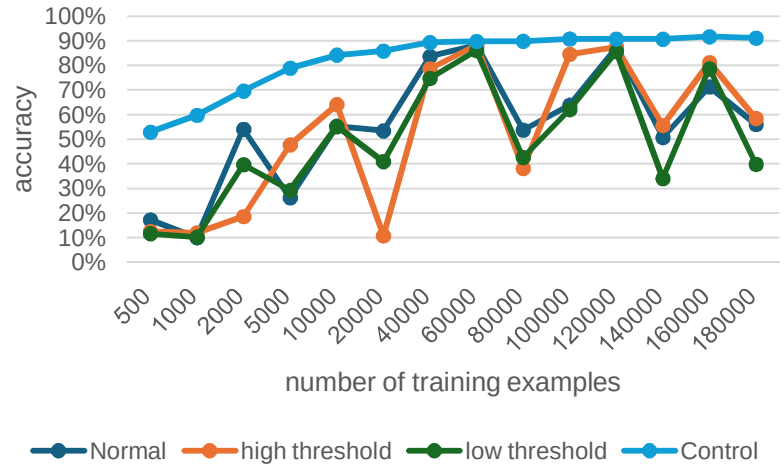

(c) Lr = 0.07

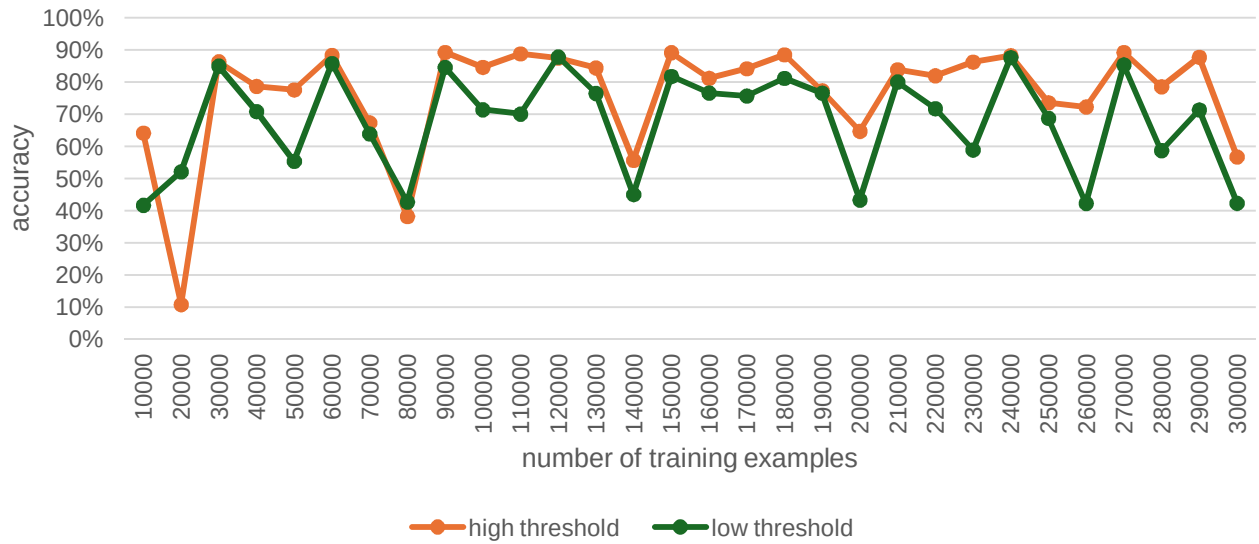

(d) Lr = 0.07

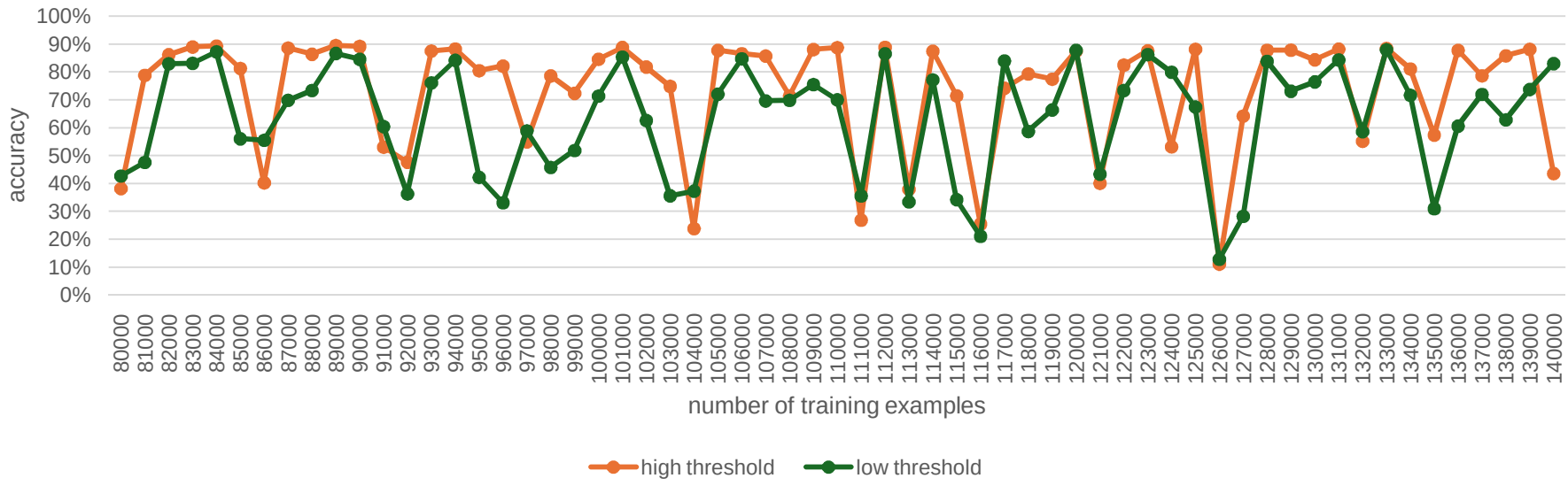
100%
90%
80%
70%
60%
50%
40%
30%
20%
10%
0%
accuracy
80000
81000
82000
83000
84000
85000
86000
87000
88000
89000
90000
91000
92000
93000
94000
95000
96000
97000
98000
99000
100000
101000
102000
103000
104000
105000
106000
107000
108000
109000
110000
111000
112000
113000
114000
115000
116000
117000
118000
119000
120000
121000
122000
123000
124000
125000
126000
127000
128000
129000
130000
131000
132000
133000
134000
135000
136000
137000
138000
139000
140000
number of training examples
high threshold
low threshold

Figure 6: Effects of KCNH7 functions in Restricted Boltzmann Machine model

(a) t = 1

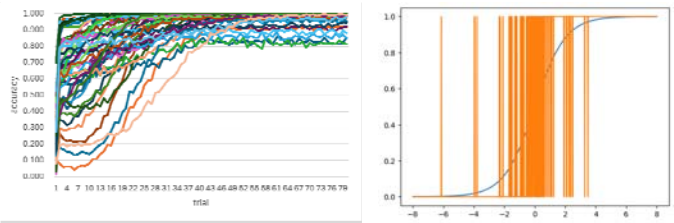

(b) t = 1/4

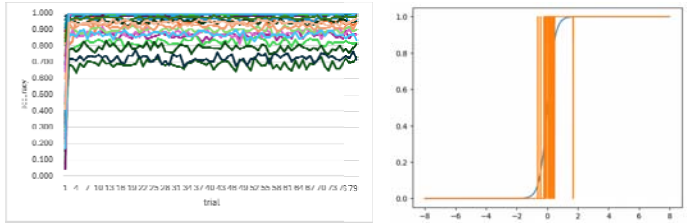

(c) t = 4

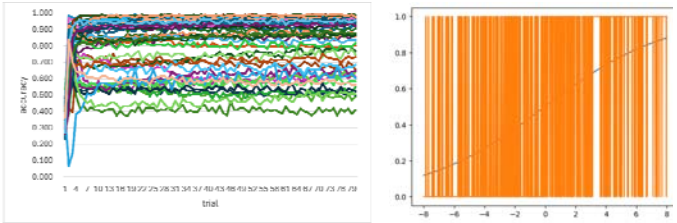

(d) Pair of numbers, t = 1

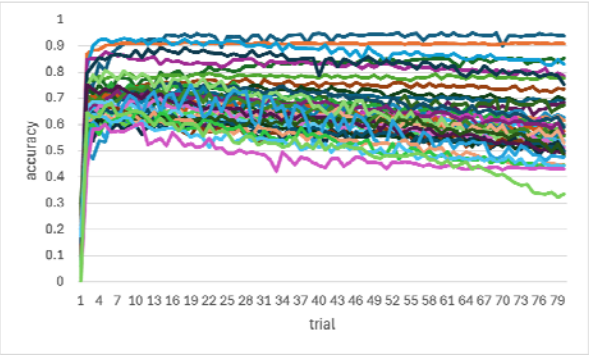

(e) Pair of numbers, t = 1/4

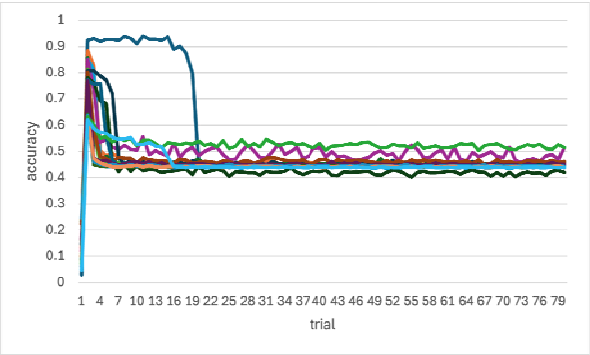

(f) Pair of numbers, t = 4

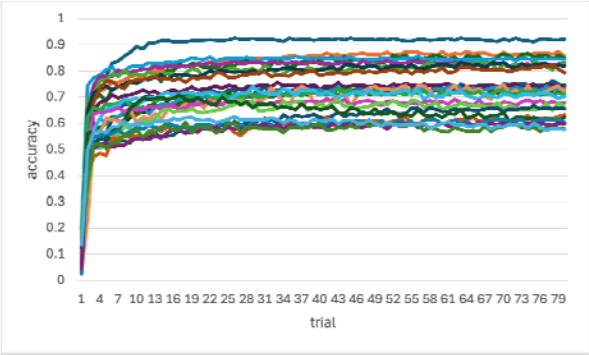

(g) Pair of numbers, t = 1/4
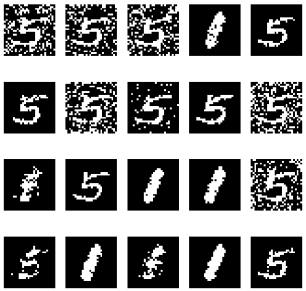
(h) Pair of numbers, t = 4